

DECAY CHARACTERISTICS OF DYSPROSIUM COMPOUND NUCLEI WITH HIGH ANGULAR MOMENTUM

G. KUMPF and V. A. KARNAUKHOV

Joint Institute for Nuclear Research

Submitted to JETP editor August 8, 1963

J. Exptl. Theoret. Phys. (U.S.S.R.) 46, 1545-1552 (May, 1964)

The energy dependences of the cross sections for the following reactions are measured: $\text{Cd}^{116}(\text{Ar}^{40}, 7n)\text{Dy}^{149}$, $\text{Cd}^{116}(\text{Ar}^{40}, 6n)\text{Dy}^{150}$, $\text{Cd}^{116}(\text{Ar}^{40}, 5n)\text{Dy}^{151}$, $\text{Cd}^{114}(\text{Ar}^{40}, 5n)\text{Dy}^{149}$, $\text{Cd}^{114}(\text{Ar}^{40}, 4n)\text{Dy}^{150}$, and $\text{Cd}^{114}(\text{Ar}^{40}, 3n)\text{Dy}^{151}$. The shape of the excitation functions is that characteristic of evaporation reactions. The experimental data are analyzed on the basis of the generalized Jackson model (at constant nuclear temperature), taking into account rotation and the limitation of possible spin values. The calculated excitation functions agree satisfactorily with experiment for the parameters $T = 3 \text{ MeV}$ and $J_{\text{cr}} = 75 \hbar$ (maximum angular momentum) and a rigid-body moment of inertia of the compound nucleus.

INTRODUCTION

It has frequently been mentioned that heavy ions possess great advantages over light bombarding particles for the purpose of investigating the behavior of a compound nucleus in a broad range of excitation energies and angular momenta. Complete coalescence and the formation of a compound nucleus is, of course, not the only process that occurs when complex nuclei interact; direct interactions can also occur. As a rule, however, it is possible to distinguish the interactions associated with compound nucleus formation and to investigate the characteristics of their decay.

When an ion and target nucleus coalesce completely the excitation energy of the compound nucleus is determined by the beam energy and the "unpacking" energy. The angular momentum is determined less definitely, because the reaction occurs with different collision parameters.

We have at present no experimental procedures for distinguishing such nuclei with definite spins. However, the same compound nucleus can be obtained from different target-projectile combinations, thus varying the spin distribution of the nuclei. The different properties of compound nuclei produced in different ways but having identical Z and A enable us to judge angular momentum effects.

The ions from C^{12} to Ne^{22} , which have thus far been used, produce compound nuclei whose angular momenta differ very little. The multiply-charged-ion cyclotron of the Joint Institute for Nuclear Research was used to accelerate the heavier argon

ions. A special operating regime of the ion source yielded a $1.5\text{-}\mu\text{A}$ current of Ar^{7+} ions and a $1\text{-}\mu\text{A}$ current of Ar^{8+} . Most of the experimental work was done with the septuply-charged ions.

The Cd^{116} and Cd^{114} targets were selected on the basis of the following considerations. In a considerable fraction of the cases the Dy^{156} and Dy^{154} compound nuclei decay emitting only neutrons, since these nuclei have a relatively high Coulomb barrier. On the other hand, fission is extremely unlikely in this nuclear region.^[1] The principal advantage of having the heavy Cd isotopes as targets is that (Ar^{40}, xn) reactions then yield α -active rare earth isotopes. Because of the limited number of α emitters in the middle of the table of isotopes, they can be identified from their half-lives without the use of chemical separation methods.

1. EXPERIMENT

Conditions of bombardment. The targets were enriched isotopes: Cd^{116} ($\text{Cd}^{116} - 72.4\%$, $\text{Cd}^{114} - 11.8\%$, $\text{Cd}^{113} - 5\%$, $\text{Cd}^{112} - 6.5\%$, $\text{Cd}^{111} - 1.3\%$, $\text{Cd}^{110} - 2.6\%$, $\text{Cd}^{108} - 0.2\%$, $\text{Cd}^{106} - 0.2\%$) and Cd^{114} ($\text{Cd}^{114} - 91.6\%$, $\text{Cd}^{116} - 1.5\%$, $\text{Cd}^{113} - 2.0\%$, $\text{Cd}^{112} - 1.3\%$, $\text{Cd}^{111} - 1.4\%$, $\text{Cd}^{110} - 0.9\%$, $\text{Cd}^{108} - 0.6\%$, $\text{Cd}^{106} - 0.7\%$).

Cadmium oxide targets were prepared by electrodeposition of $\text{Cd}(\text{NO}_3)_2$ from an organic medium. The nitrate was converted into an oxide by heating. The target backing was 0.7-mg/cm^2 aluminum foil. By weighing on a microbalance the total amount of matter was determined to be 1 mg/cm^2 . By comparing the initial weight of the

cadmium with the weight of the deposit and of the matter remaining in solution it was shown that the targets actually consisted of CdO.

The irradiation took place within a special sample holder in the internal cyclotron beam, which impinged on the CdO layer. The recoil nuclei traversed the target backing and were stopped in a stack of thin aluminum collectors 0.6–0.7 mg/cm² thick. The target and collectors were held in a cooled cassette.

In preliminary runs the ranges of dysprosium recoil nuclei were measured with a thin (80 μg/cm²) target and thin (300 μg/cm²) collectors; the depth of penetration in aluminum was found to obey a strict Gaussian law. At the recoil energy $E_R = 64$ MeV (for 258-MeV incident-ion energy) the mean Dy range in Al was $\bar{R} = 2.40$ mg/cm² with the mean spread $\Delta R = 0.34$ mg/cm².

Figure 1 shows the range-energy curve for Dy and Tb, based on [2] up to 30 MeV and on the present work at higher energies. Energies were calculated assuming total momentum transfer.

The argon ions traversed the target and the stack of foils before reaching the collector. The number of incident ions was determined from the collector current taking into account the effective (equilibrium) charge of argon atoms calculated from the data in [3]. Since the equilibrium charge was not known with sufficient accuracy, the stack of foils behind the target was made thick enough so that in all runs the argon ions reached the collector with approximately the same energy, the effective charge being the fraction 0.6–0.7 of the argon ionic charge. In this way good relative accuracy was attained in measuring the number of ions in experimental runs at different energies. Inaccuracy in determining the effective charge could be avoided in principle if the target could be fastened to the collector; in this case the true Ar⁷⁺ or Ar⁸⁺ current would be measured. In our case, however, the measurements were distorted by ions with charges < 7 accelerated at high-frequency harmonics.

The argon ion energy was measured with a semiconductor detector. A part of the beam passed through a small aperture in the collector and was scattered in gold foil 0.1 μ thick; ions scattered at 13° reached the detector. Pulses from the detector were fed through a preamplifier and amplifier to a 100-channel analyzer. The energy was measured by comparing the amplitudes of Ar⁴⁰ ions and α particles from a Th (C + C') source. The half-width of the ion lines was usually 6%, but it can be stated that the beam itself was considerably more monoenergetic. The experimental energy was

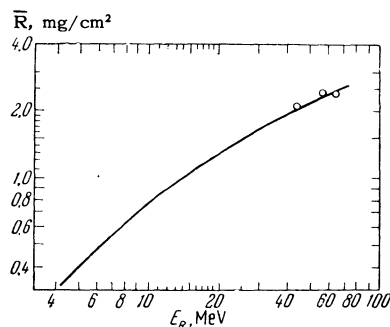


FIG. 1. Mean range \bar{R} of Dy in Al vs. recoil energy E_R .

varied by changing the radius at which the target was placed.

Method of registration. After each bombardment the stack of collectors was dismantled, and decay curves were recorded using α counters with ZnS crystals. After the short-lived activity had decayed, each sample was placed in a gridded α chamber for an absolute calibration of the counters; corrections were introduced for the sample thickness. The accuracy of the absolute count exceeded 5%. An electronic computer using the method of least squares decomposed the decay curves into components with the half-lives 17.9 min (Dy¹⁵¹), 7.4 min (Dy¹⁵⁰), and 4.1 hr (Tb¹⁴⁹). The statistical errors of the expansion coefficients were usually under 5%; no activities with different half-lives were observed. In calculating the cross sections it was considered that α decay of Dy¹⁵¹, Dy¹⁵⁰, and Tb¹⁴⁹ occurs in 6.2, 17.9, and 10% of all cases respectively. [4]

In [4] it was noted that the cross sections for reactions in which Tb¹⁴⁹ is formed from Tb compound nuclei are negligibly small compared with similar reactions for other nuclei. This results from the fact that Tb¹⁴⁹ has an isomeric state, [5] which decays with a half-life of 4 min, emitting an α particle. This isomer "screens" the ground-state in the reactions. It can therefore be assumed that all of the Tb¹⁴⁹ observed by us results from K capture or β⁺ decay of Dy¹⁴⁹. Regarding the properties of Dy¹⁴⁹ decay it is only known that the lifetime is short. Unfortunately, there are no direct measurements of the relative probability of Dy¹⁴⁹ decay into the isomeric and ground states of Tb¹⁴⁹. However, an estimate can be obtained from the yield of the respective reactions. We measured the cross sections for the reactions Cd¹¹⁶(Ar⁴⁰, 5n) Dy¹⁵¹ and Cd¹¹⁴(Ar⁴⁰, 5n) Dy¹⁴⁹ → Tb¹⁴⁹. The terbium yield in the second reaction was approximately 2.5 times smaller than the Dy¹⁵¹ yield in the first reaction, but the excitation functions behave alike. Similar observations are given in [4].

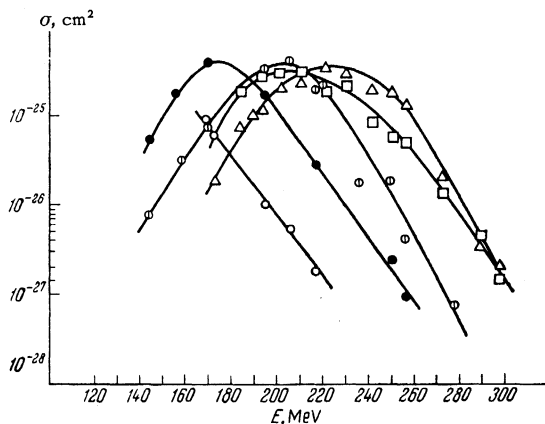


FIG. 2. Cross section vs. incident-ion energy (lab. system) for the reactions: Δ - $\text{Cd}^{116}(\text{Ar}^{40}, 7n)\text{Dy}^{149}$, \circ - $\text{Cd}^{114}(\text{Ar}^{40}, 5n)\text{Dy}^{149}$, \circ - $\text{Cd}^{114}(\text{Ar}^{40}, 3n)\text{Dy}^{151}$, \square - $\text{Cd}^{116}(\text{Ar}^{40}, 6n)\text{Dy}^{150}$, \bullet - $\text{Cd}^{114}(\text{Ar}^{40}, 4n)\text{Dy}^{150}$.

It can therefore be asserted that only about 40% Dy^{149} is transformed into the ground state of Tb^{149} . This was taken into account in calculating the Dy^{149} yield. The absolute cross sections for reactions in which Dy^{149} is formed are, of course, less accurate than the other cross sections.

Experimental results. Figure 2 shows the measurements of cross sections for different reactions as functions of argon ion energy. Figure 3 gives the excitation functions plotted from the data in Fig. 2. The ordinate is the probability that x neutrons are emitted, which is $F_x = \sigma_{xN}/\sigma_0$, where σ_{xN} is the cross section for a reaction with the emission of x neutrons, σ_0 is the total cross section, and $x = 3-7$. The values of the total cross sections were taken from the calculations in [6] based on a sharply bounded black nuclear model of radius $r_0 = 1.45 \times 10^{-13}$ cm. These cross sections differ only slightly from the classical cross

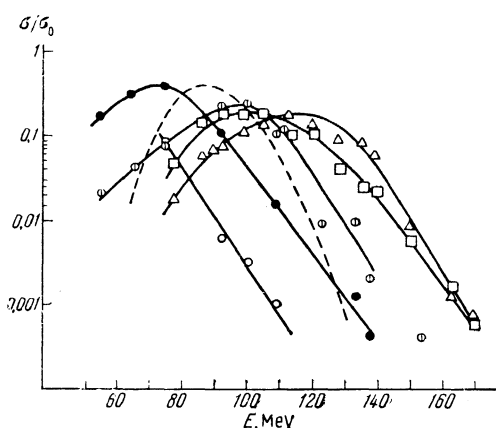


FIG. 3. Probability of neutron emission, $F_x = \sigma_x/\sigma_0$. The abscissa is the compound-nucleus excitation energy (with the same notation as in Fig. 2). The dashed curve is the excitation function for the reaction $\text{Nd}^{144}(\text{C}^{12}, 6n)\text{Dy}^{150}$. [8]

sections calculated using the formula

$$\sigma_0 = \pi(R_1 + R_2)^2(1 - V/E),$$

where R_1 and R_2 are the radii of the colliding nuclei, V is the height of the Coulomb barrier, and E is the projectile energy. The mass defect (52 MeV) in the reaction was calculated using the mass tables in [7].

It should be noted that as the energy decreases below the maximum for any reaction the effect of the light cadmium isotopes gradually becomes evident. Therefore the excitation functions in Fig. 3 are given only in the energy range where the effect on the principal isotope could be distinguished reliably.

2. ANALYSIS OF EXPERIMENTAL DATA

A few qualitative remarks are in order before we proceed to analyze the results. The experiments furnish no direct proof that all neutrons are emitted by evaporation from a uniformly heated compound nucleus. The data on the ranges of recoil nuclei are consistent with a total transfer of Ar momentum to the compound system. However, the measurements are not sufficiently accurate to permit the observation of any reduction of the range due to the ejection of some neutrons through direct interactions. Experiments using other projectiles ($\text{C}^{12}-\text{Ne}^{20}$) to study excitation functions for reactions accompanied by neutron emission, [8] and investigations of spectra and neutron angular distributions [9] suggest that in reactions leading only to neutron emission the dominant mechanism is the decay of a compound nucleus.

The general picture of the decay of a rotating compound nucleus has been discussed frequently (see [10], for example). The excitation energy of a rotating nucleus can be represented as consisting of "thermal" and "collective" parts: $E = E_T + E_C$. The collective energy is determined by the rotational and deformation energies: $E_C = E_R + \Delta(E_Q + E_S)$. Neutron evaporation reduces mainly the thermal portion of the excitation energy, since each neutron carries away only a small fraction of the total nuclear angular momentum. In [8] the mean angular momentum of a neutron is estimated to be not more than $3\hbar$. The remaining angular momentum is removed through the emission of a γ -ray cascade, the existence of which has been proved in several experimental papers.

Our calculation of the excitation functions for (Ar^{40}, xn) reactions was based on this picture, assuming that the evaporation of a given number of neutrons depends on the magnitude of E_T . It is

qualitatively clear how the excitation function should vary as the angular momentum of a nucleus increases. The presence of collective energy associated with rotation should shift the excitation function maxima toward higher energies and increase their half-widths. This results from the fact that a given value of E_T can be realized in a broader range of excitation energies due to the E_C contribution. Figure 3 shows the excitation functions for the evaporation of five neutrons, obtained in reactions with ions lighter than Ar. These functions are, indeed, narrower and located in a lower range of excitation energies.

The calculation was based on the Jackson model,^[11] which was proposed to explain the cross sections for (p, xn) reactions. The calculational scheme was extended to the case of a compound nucleus with high angular momentum. The main assumptions and the initial formulas of the calculation follow.

A. It is assumed that the spins J of the compound nuclei have a classical distribution represented by

$$w(J) dJ = \frac{2J}{J_{max}^2} dJ \quad \text{for } J < J_{max}$$

$$= (R_1 + R_2) \sqrt{2\mu(E - V)},$$

$$w(J) = 0 \quad \text{for } J > J_{max} \quad (1)$$

(μ is the reduced mass). A comparison of (1) with the distributions obtained from quantum-mechanical calculations^[6] in the case of such heavy particles as Ar⁴⁰ has shown that (1) is a good approximation.

B. It is assumed that rotation does not seriously deform a nucleus and does not change the sum of Coulomb and surface energies, i.e., $E_C = E_R = J^2/2I$, where I is the moment of inertia of a rigid spherical nucleus. The J distribution for a given excitation energy is easily converted into an E_R distribution:

$$w(E_R) dE_R = dE_R/E_{Rmax}, \quad \text{if } E_R < E_{Rmax} = J_{max}^2/2I;$$

$$w(E_R) = 0, \quad \text{if } E_R > E_{Rmax}. \quad (2)$$

C. We assume, as did Jackson,^[11] that the nuclear temperature T is constant at all stages of the neutron cascade. Then the probability that the internal energy $E_T = E - E_R$ is carried away by x neutrons can be represented approximately by

$$P(E_T, x) = I(\Delta_x, 2x - 3) - I(\Delta_{x+1}, 2x - 1) \quad \text{for } \sum_{i=1}^{x+1} B_i < E_T,$$

$$P(E_T, x) = 0 \quad \text{for } E_T < \sum_{i=1}^{x+1} B_i. \quad (3)$$

Here

$$\Delta_x = (E_T - \sum_{i=1}^x B_i)/T, \quad \Delta_{x+1} = (E_T - \sum_{i=1}^{x+1} B_i)/T,$$

B_i is the binding energy of the i -th neutron, and

$$I(z, n) = \frac{1}{n!} \int_0^z x^n e^{-x} dx$$

is an incomplete Γ function. From (3) and (2) we obtain the probability that x neutrons are emitted at excitation energy E :

$$F_x = \int_0^{E_{Rmax}} w(E_R) P(E - E_R, x) dE_R$$

$$= \frac{1}{E_{Rmax}} \int_{E - E_{Rmax}}^E P(E_T, x) dE_T, \quad (4)$$

where $P(E_T, x)$ is determined from (3).

The integrals with respect to the first variable of the incomplete Γ functions were obtained numerically by means of tables.^[12] The probabilities F_x calculated in this way were found to decrease very slowly at high energies (curve 2 of Fig. 4). This result is associated with the fact that the mean internal energy \bar{E}_T increases weakly with increasing excitation energy due to the contribution of the rotational energy.

D. In connection with the foregoing we introduce a limitation on the possible spins of the compound nuclei. It is assumed that the compound nuclei are not formed with angular momentum above a certain critical amount J_{cr} . There are several reasons for this. It is known that in the case of grazing collisions there is a high probability of nucleon transfer and partial amalgamation. As a result, states with angular momentum close to J_{max} are not included in the process of compound nucleus formation. Also, it follows from calculations based

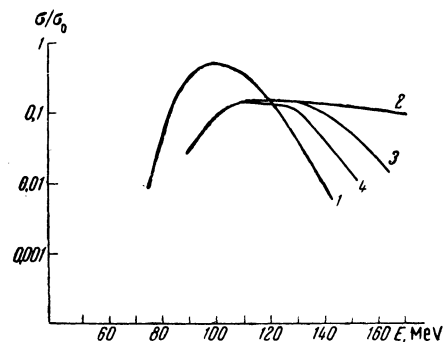


FIG. 4. Calculated probabilities of emitting seven neutrons. Curve 1 - neglecting rotation; 2 - including rotation, without spin cutoff; 3 - including rotation and spin cutoff at $J_{cr} = 100\hbar$; 4 - with spin cutoff at $J_{cr} = 75\hbar$, $T = 3$ MeV. The nuclear moment of inertia is taken to be that of a rigid body.

on the liquid-drop model^[13] that compound nuclei cannot be formed with angular momentum greater than a critical amount because an equilibrium shape does not then exist. In the calculations the spin cutoff is taken into account simply by the fact that at the lower boundary of the second integral in^[4] E_{\max} cannot assume values greater than $E_{\text{CR}} = J_{\text{CR}}^2/2I$. Therefore the probabilities $F_X = \sigma_{\text{XN}}/\sigma_0$ depend on three parameters—the temperature T , the effective moment of inertia I , and the critical angular momentum J_{CR} .

Figure 4 represents the probability F_7 of the evaporation of seven neutrons as a function of the excitation energy for several choices of the parameters. Curve 1 was calculated from Jackson's formula neglecting collective energy. When rotation is taken into account the curves are shifted to the right and become flatter and broader. Without the introduction of spin cutoff (curve 2) the excitation function declines only insignificantly at high energies. When cutoff is included there is a sharper drop at high energies, and J_{CR} determines the position of the upper limit (curves 3 and 4). The left-hand limits of the curves depend on temperature. The variation of the moment of inertia changes mainly the vertical positions of the curves.

The closest agreement between the calculated and measured probabilities of all reactions was obtained using the following parameters: $T = 3$ MeV, rigid-sphere moment of inertia $I = \frac{2}{5}R^2M$ (R is the radius of the compound nucleus), and $J_{\text{CR}} = 75\hbar$. Figure 5 shows curves calculated using these parameters.

The calculated and experimental excitation functions are in satisfactory agreement with regard to the shapes of the curves and the absolute probabilities of the reactions. The proposed simple model for calculating the probabilities of neutron evaporation from rotating compound nuclei is obviously correct in general. It is absolutely necessary to introduce a spin cutoff in this type of calculation, without claiming any great accuracy in determining J_{CR} . A comparison of curves 3 and 4 in Fig. 4 shows how sensitive the curve shape is to the value of J_{CR} . A comparison of the calculations with experiment does not yield J_{CR} with greater than 20% accuracy. Also, the considered model does not take into account the deformation of a rotating nucleus, which makes the collective energy deviate from quadratic dependence on the spin. J_{CR} is obviously increased somewhat when the nuclear deformation is taken into account.

The authors consider it their pleasant obligation to thank G. N. Flerov for encouragement in the course of the experimental work. Professor

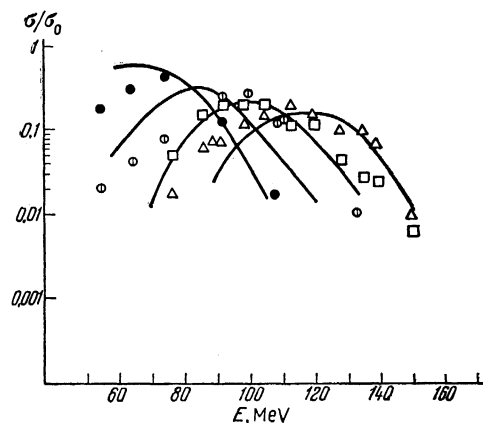


FIG. 5. Calculated probabilities with $T = 3$ MeV and $J_{\text{CR}} = 75\hbar$ (for a rigid-body nuclear moment of inertia). The experimental points are given for the same reactions as in Fig. 2.

I. Schintlmeister and K. Kaufmann of the Central Institute for Nuclear Investigations at Rossendorf are thanked for their kindness in providing silicon detectors. The authors are indebted to the cyclotron crew and to A. S. Pasyuk and I. A. Shelaev for the uninterrupted operation of the cyclotron, and to E. A. Loginova for the electronic computer calculations.

¹ Gilmore, Thompson, and Perlman, Phys. Rev. 128, 2276 (1962).

² J. M. Alexander and D.H. Sisson, UCRL 10098, 1962.

³ F. W. Martin and L. C. Northcliffe, Phys. Rev. 128, 1166 (1962).

⁴ G. N. Simonoff and J. M. Alexander, UCRL 10099, 1962.

⁵ R. D. Macfarlane, Phys. Rev. 126, 274 (1962).

⁶ V. V. Babikov, JETP 38, 274 (1960), Soviet Phys. JETP 11, 198 (1960).

⁷ A. G. W. Cameron, Can. J. Phys. 35, 1021 (1957).

⁸ J. M. Alexander and G. N. Simonoff, UCRL 10541, 1962.

⁹ H. W. Broek, Phys. Rev. 124, 233 (1961).

¹⁰ G. N. Flerov and W. A. Karnaukhov, Proc. of the Conf. on Direct Interactions and Nuclear Reaction Mechanisms, Gordon and Breach, 1963, p. 901.

¹¹ J. D. Jackson, Can. J. Phys. 34, 767 (1956).

¹² E. E. Slutskii, Tablitsy nepolnoĭ Γ -funktsii (Tables of the Incomplete Gamma Function), AN SSSR, 1950.

¹³ G. A. Pik-Pichak, JETP 34, 341 (1958), Soviet Phys. JETP 7, 238 (1958).

Translated by I. Emin